Journal of Alloys and Compounds 502 (2010) 401–406

Contents lists available at ScienceDirect

Journal of Alloys and Compounds

journal homepage: www.elsevier.com/locate/jallcom

Effect of MgO nanolayer coated on $Li_3V_2(PO_4)_3$/C cathode material for lithium-ion battery

Jing Zhai [a], Minshou Zhao [a,b,*], Dandan Wang [a], Yuqing Qiao [a]

[a] Provincial Key Laboratory of Applied Chemistry, College of Environmental and Chemical Engineering, Yanshan University, Qinhuangdao 066004, PR China
[b] State Key Laboratory of Metastable Material Science and Technology, Yanshan, University, Qinhuangdao 066004, PR China

ARTICLE INFO

Article history:
Received 21 January 2010
Received in revised form 20 April 2010
Accepted 25 April 2010
Available online 4 May 2010

Keywords:
Sol–gel
Magnesium oxide
Nanocoating
Electrochemical performance
Cathode material
Lithium-ion battery

ABSTRACT

MgO nanolayer coated on $Li_3V_2(PO_4)_3$/C particles was successfully prepared by a sol–gel method. The X-ray diffraction (XRD) shows that the crystal structure of the $Li_3V_2(PO_4)_3$/C cores does not been affected by the coating. Nanolayer-structured MgO on the surface of $Li_3V_2(PO_4)_3$/C particles is demonstrated by high resolution transmission electron microscopy (HRTEM). Galvanostatic charge/discharge, EIS and cyclic voltammetry measurements clearly show that MgO nanocoating stabilizes the structure of the cathode material, decreases the interface charge transfer resistance and enhances the reversibility of electrode reaction. Electrochemical properties of the coated samples were investigated, showing enhancements of the initial discharge capacity, the cyclability and the rate performance. For MgO of 4.5 mol% coated sample, the initial discharge capacity is 194.4 mAh g^{-1} at 40 mA g^{-1} current density, which is close to the theoretical discharge capacity of 197 mAh g^{-1}, and the discharge capacity remains 137.5 mAh g^{-1} after 100 cycles, and its capacity retention of 70.73% is higher than that of pristine $Li_3V_2(PO_4)_3$/C, 43.7%. The initial discharge capacity still reaches 157.81 mAh g^{-1}, 157.29 mAh g^{-1} and 144.64 mAh g^{-1} at 1C, 1.5C, 2C rates, respectively.

1. Introduction

Rechargeable lithium-ion batteries are considered as one of the most advanced energy storage systems. Currently, $LiCoO_2$ is widely used as cathode material in commercial lithium-ion batteries [1], but its high cost, safety and toxicity inhibit its use in large-scale and biomedical application, so more efforts have been made to explore novel cathode material. In recent years, as part of efforts for identifying new cathode material for rechargeable lithium batteries, lithiated transition metal phosphates such as $LiFePO_4$ [2,3], $LiCoPO_4$ [4], $LiMnPO_4$ [5,6] and $Li_3V_2(PO_4)_3$ [7–9] have attracted significant interests due to their good lithium ion mobility, high reversible capacity, operative redox potentials and high safety. Among all the phosphates, monoclinic lithium vanadium phosphate ($Li_3V_2(PO_4)_3$, LVP) is a highly promising cathode material proposed for lithium ion batteries, which shows an average intercalation voltage up to 4.0 V and a theoretical capacity of 197 mAh g^{-1}.

However, it is well known that low electronic conductivity of LVP affects its electrochemical properties greatly [10], especially the fast rate performance. In most of the early reports, many efforts including metal doping [11–14], coating with carbon [15,16] and mixing the precursor with some conductive metal powders [17] have been made to improve the performances of $Li_3V_2(PO_4)_3$ cathode material. In addition to, it has been reported that ZrO_2 coated $LiFePO_4$ remarkably enhanced the electrochemical performances of LiFePO4 cathode material [18]. However, up to now, there has been no report yet on metal oxide coated on $Li_3V_2(PO_4)_3$ particle surface. In this work, MgO nanolayer coated on $Li_3V_2(PO_4)_3$/C cathode material by sol–gel method was performed and the resultant electrochemical performances are reported.

2. Experimental

The pristine $Li_3V_2(PO_4)_3$/C was synthesized by a sol–gel method.$V_2O_5{\cdot}nH_2O$ hydro-gel was prepared as follows: 10% (v/v) H_2O_2 solution was slowly added to V_2O_5, while vigorously stirred in ice-water until a clear orange solution formed, and then brownish homogeneous V_2O_5 gels were obtained after 4 h at 35 °C. Aqueous solution of the stoichiometric $NH_4H_2PO_4$, $CH_3COOLi{\cdot}2H_2O$ and citric acid were added to the above $V_2O_5{\cdot}nH_2O$ hydro-gels, respectively. The mixtures were heated gently with continuous stirring to remove the excess water at 80 °C until the blue precursor was obtained, which was dried in a vacuum oven at 80 °C for 12 h to get resultant powder, and then the powder sample was ground in an agate mortar, pelletized and heated at 300 °C in a furnace with flowing nitrogen gas for 4 h to allow the formation and release of NH_3 and H_2O. Thereafter temperature was risen to 800 °C at a rate of 15 °C min^{-1} and kept for 5.5 h with a stream of nitrogen gas. The sample was taken out and ground in an agate mortar when the temperature was fallen down to room temperature, getting particle size span from 0.5 to 4 μm, which was used as pristine material, and $Mg(CH_3COO)_2{\cdot}4H_2O$ was used as coating reagent. $Li_3V_2(PO_4)_3$/C powder was initially dispersed into ethanol containing the desired amount of $Mg(CH_3COO)_2{\cdot}4H_2O$ by a blender and followed by an ultrasonic stirring

* Corresponding author. Tel.: +86 3358074730; fax: +86 3358061569.
E-mail addresses: Zhaijing1975@163.com (J. Zhai), zhaoms@ysu.edu.cn (M. Zhao).

0925-8388/$ – see front matter © 2010 Elsevier B.V. All rights reserved.
doi:10.1016/j.jallcom.2010.04.181

for 10 min, then dried with a rotary evaporator under reflux condition. The residue as-obtained was slightly ground, pressed into pellets, and then sintered at 650 °C for 4 h in flowing N_2 atmosphere to decompose the organic radicle and create a MgO coating layer on the particle surface of $Li_3V_2(PO_4)_3$/C. The coated amount of MgO on $Li_3V_2(PO_4)_3$/C powders was 3.5, 4.0, 4.5 and 5.0 mol%, respectively.

X-ray diffraction (XRD) was performed on $Li_3V_2(PO_4)_3$/C powders before and after coated using a D/Max-2500/PC X-ray diffractometer (Cu Kα radiation). The surface morphology of powder $Li_3V_2(PO_4)_3$/C coated and uncoated with MgO was observed by a Hitachi S-4800 scanning electron microscopy instrument (SEM), respectively. The microstructures of the coated particles were examined by a JEM-2010 transmission electron microscope.

Electrochemical performances of the samples were evaluated in columned test cells. To prepare the electrodes used for the electrochemical performances measurement, the powders of pristine $Li_3V_2(PO_4)_3$/C and MgO coated $Li_3V_2(PO_4)_3$/C were mixed with acetylene black and polyvinylidine fluoride (PVDF) binder in a weight ratio of 80:15:5 in *N*-methyl-2-pyrrolidone (NMP) to ensure the homogeneity, respectively. The obtained slurry was coated on Al foil, dried under the infrared light and cut into foursquare strips of 8 mm × 8 mm in size, and the calculation to mass of active materials is carried out by the difference between the mass of active material coated Al foil and the mass of pristine Al foil to multiple 80%. After the strips were dried at 120 °C for 12 h in a vacuum, two-electrode electrochemical cells were assembled in a Mikrouna glove box filled with high-purity argon where the lithium metal foil was used as anode, Celgard® 2320 as separator, and 1 M $LiPF_6$ in EC: DMC (1:1 vol.%) was used as electrolyte, and then charge/discharge test was carried out using a Neware Battery Tester. The electrochemical measurements were performed in the voltage range of 3.0–4.8 V at room temperature. EIS measurements were carried out in three-electrode cells by using CHI 660A electrochemical analyzer (Chenhua, Shanghai, China) with a ±5 mV ac signal and a frequency range from 10^5 to 10^{-2} Hz. Cyclic voltammograms were obtained on a ZF-9 potentiostat by scanning electrode potential at the rate of 5 mV min^{-1} between 3.0 and 4.8 V.

3. Results and discussion

The XRD patterns of pristine $Li_3V_2(PO_4)_3$/C and MgO coated $Li_3V_2(PO_4)_3$/C are presented in Fig. 1, in which All diffraction lines can be indexed to the monoclinic structure with space group 14($P2_1/n$) and are consistent with the published results [19].Additionally, peak shift is not observed before and after the surface modification by MgO within the detectable limit of XRD, and no peaks related to MgO are observed in the XRD patterns of the MgO-modified samples, which is consistent with the result reported in literature [20]. However, the lattice parameter decreases slightly from the value of the uncoated material (a = 8.569 Å, b = 8.636 Å) to the value of 4.5 mol% MgO coated $Li_3V_2(PO_4)_3$/C (a = 8.552 Å, b = 8.624 Å). Taking into account the ionic radius of Mg^{2+} (0.72 Å) smaller than that of V^{3+} (0.74 Å), such an decrease suggests that a small amount of Mg^{2+} ions can be incorporated into the monoclinic structure by soft re-heating, which is similar to previously reported results [20,21]. Because of the controlled reaction time, we believe that only a thin layer of solid solution $Li_3Mg_xV_{2-x}(PO_4)_3$ was formed on the surface of the $Li_3V_2(PO_4)_3$/C particles. Therefore, no traces of solid solution were detected with XRD.

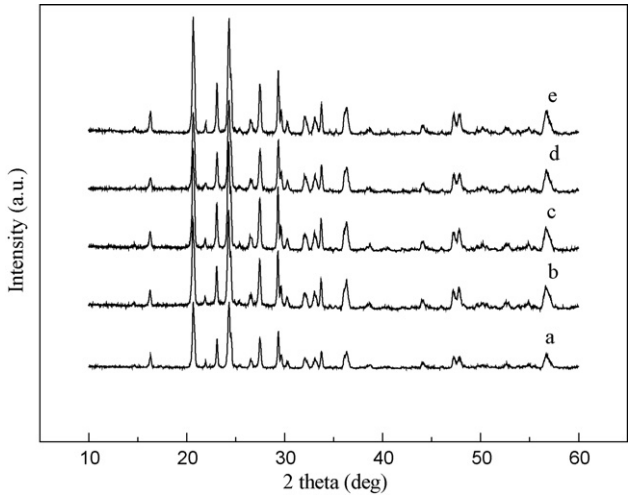

Fig. 1. XRD patterns of $Li_3V_2(PO_4)_3$/C (a) and MgO coated $Li_3V_2(PO_4)_3$/C 3.5 mol% (b), 4.0 mol% (c), 4.5 mol% (d) and 5.0 mol% (e).

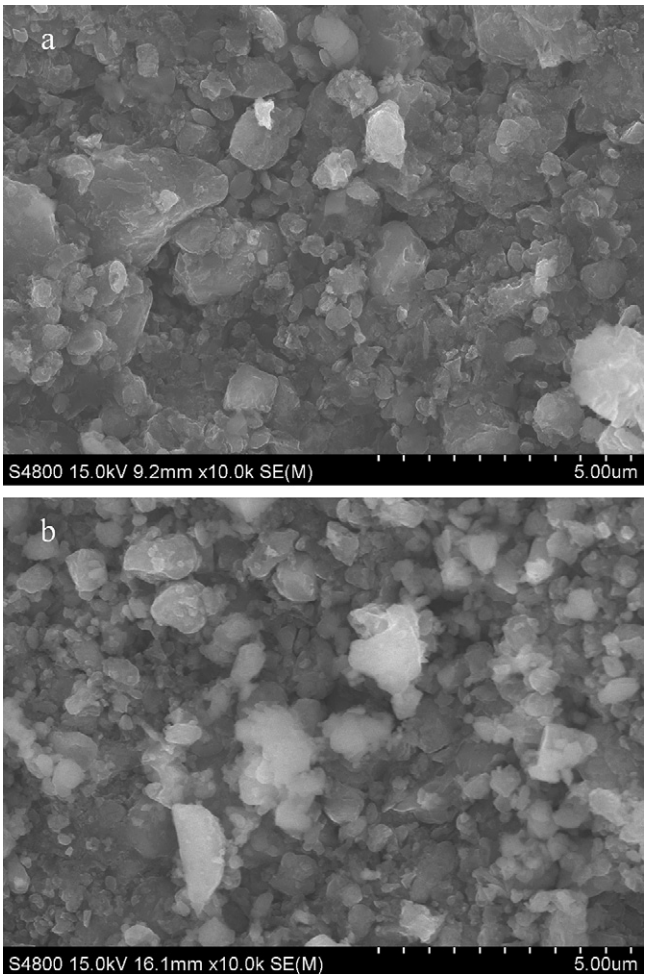

Fig. 2. Morphology of $Li_3V_2(PO_4)_3$/C (a) and 4.5 mol% MgO coated $Li_3V_2(PO_4)_3$/C (b).

The morphology of pristine $Li_3V_2(PO_4)_3$/C and MgO coated $Li_3V_2(PO_4)_3$/C were observed by SEM. Fig. 2 shows that the size of the particles of uncoated $Li_3V_2(PO_4)_3$/C is un-uniform. After coated with MgO of 4.5 mol%, the particles do not show obvious change in morphology except for being more homogeneous in particle size distribution.

The microstructure of MgO coated $Li_3V_2(PO_4)_3$/C particle was analyzed by high resolution TEM(Fig. 3), which confirms that MgO is coated on the surface of $Li_3V_2(PO_4)_3$/C. This HRTEM image clearly illustrates that the thickness of MgO coating layer is about 2.0–2.5 nm and the lattice fringe spacing of $Li_3V_2(PO_4)_3$/C is 0.36 nm. We performed EDS spot analysis at the coating layer, detecting the presence of Mg and O. The figure of EDS and the results of EDS analysis in atom % are shown in Fig. 4 and Table 1, respectively. This confirms that the coating consists of MgO film.

The second charge/discharge curves are shown in Fig. 5 for pristine $Li_3V_2(PO_4)_3$/C and MgO of 4.5 mol% coated $Li_3V_2(PO_4)_3$/C test cells at 40 mA g^{-1} current density in the range of 3.0–4.8 V at room temperature. It can be seen that the profiles of the charge/discharge curves for the two samples are almost the same. Four plateaus appear in the charge process and three plateaus in the discharge process, which consistent with the results [22], but the charge/discharge plateaus are longer for MgO coated $Li_3V_2(PO_4)_3$/C. From the second charge/discharge curves, the

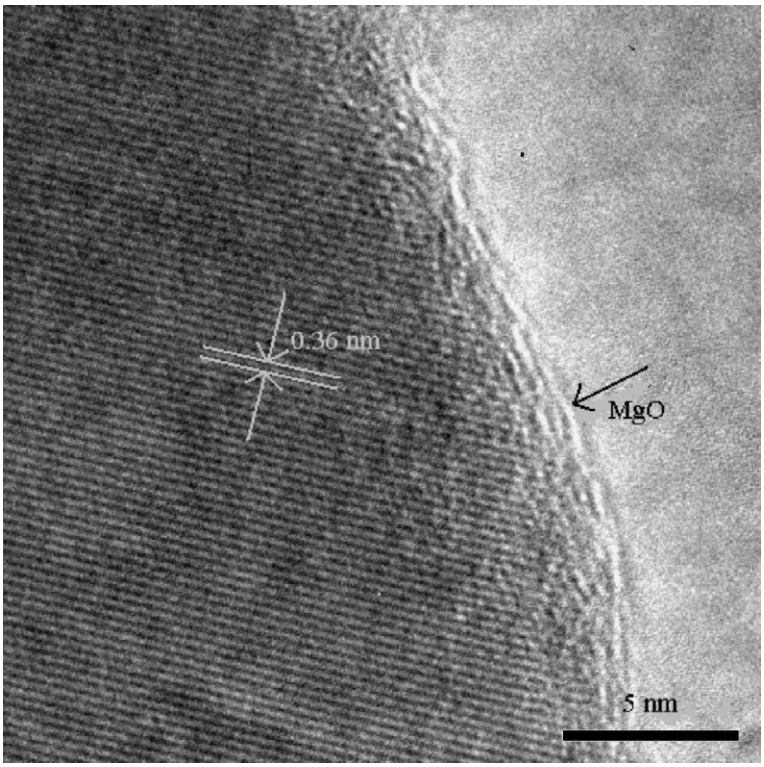

Fig. 3. TEM image of 4.5 mol% MgO-coated $Li_3V_2(PO_4)_3$/C.

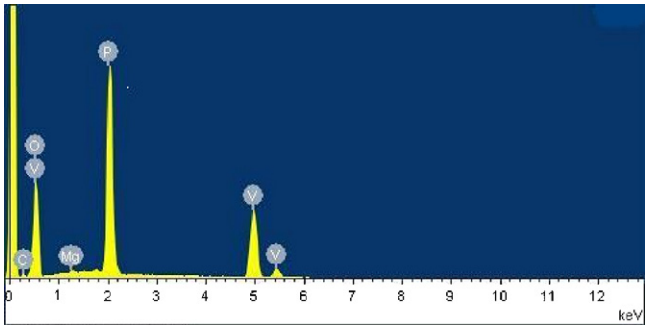

Fig. 4. EDS image of 4.5 mol% MgO-coated $Li_3V_2(PO_4)_3$/C.

effects of modification with MgO are not so apparent, but the significant effects can be observed from the long-term charge/discharge cycle in the following tests, such as the twentieth charge/discharge curves of pristine $Li_3V_2(PO_4)_3$/C and the thirtieth charge/discharge curves of MgO of 4.5 mol% coated $Li_3V_2(PO_4)_3$/C (Fig. 6). It is obvious that the profile of discharge curve was changed for pristine $Li_3V_2(PO_4)_3$/C, the first two discharge plateaus of pristine $Li_3V_2(PO_4)_3$/C were merged into one, and two discharge plateaus appear in the discharge process only. However, the discharge curve profile of MgO coated $Li_3V_2(PO_4)_3$/C is not altered and there are still three discharge plateaus in the discharge process. This

Table 1
Results of EDS analysis.

Element	Weight (%)	Atom (%)
C	4.34	7.98
O	45.89	63.45
Mg	0.32	0.30
P	24.32	17.36
V	25.13	10.91

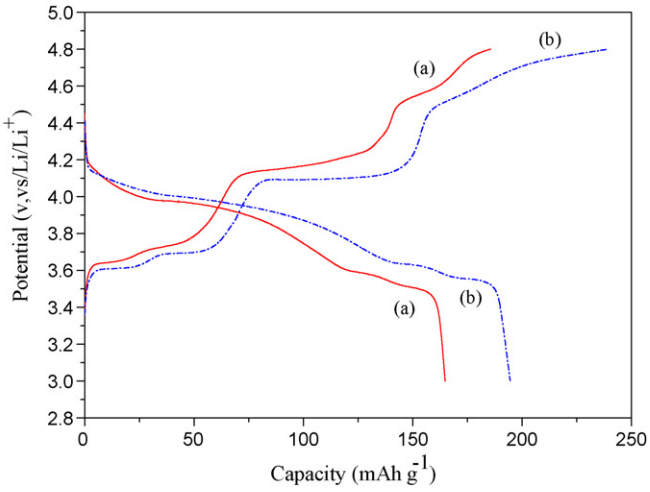

Fig. 5. Second charge/discharge curves of $Li_3V_2(PO_4)_3$/C (a) and 4.5 mol% MgO coated $Li_3V_2(PO_4)_3$/C (b).

demonstrates that the MgO coating suppresses the microstructure change of $Li_3V_2(PO_4)_3$/C caused by repetition of lithium-ion insertion–extraction reaction, and thus improves structural stability of the cathode material.

EIS measurements were performed on pristine $Li_3V_2(PO_4)_3$/C and MgO of 4.5 mol% coated $Li_3V_2(PO_4)_3$/C electrodes, respectively. The electrodes were galvanostatically charged/discharged for 10 cycles to ensure the stable formation of the SEI layers on the surface of the electroactive particles. The EIS was then measured in the fully discharged state. EIS and an equivalent circuit [23] are shown in Figs. 7 and 8, respectively. EIS data were fitted using Zview-Impedance 2.80 software. Fig. 7 shows typical Nyquist plots of pristine $Li_3V_2(PO_4)_3$/C and MgO coated $Li_3V_2(PO_4)_3$/C composite electrodes. The plots show an intercept at high frequency, followed

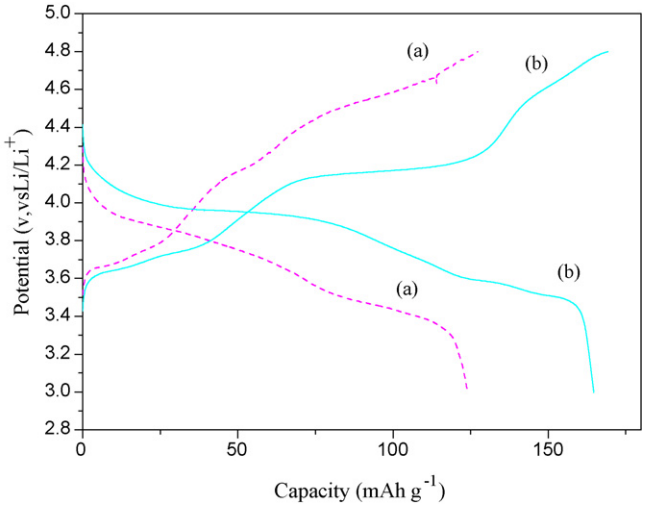

Fig. 6. Charge/discharge curves of $Li_3V_2(PO_4)_3$/C (twentieth) (a) and 4.5 mol% MgO coated $Li_3V_2(PO_4)_3$/C (thirtieth) (b).

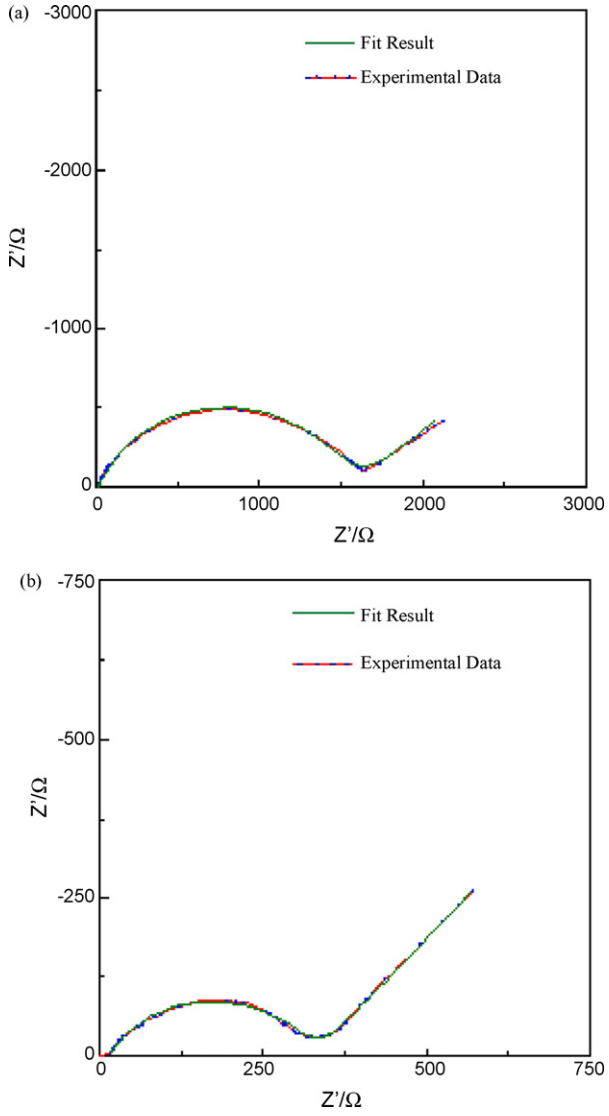

Fig. 7. EIS of $Li_3V_2(PO_4)_3$/C(a) and 4.5 mol% MgO coated $Li_3V_2(PO4)_3$/C (b). Fitting lines show fitted results from equivalent circuit.

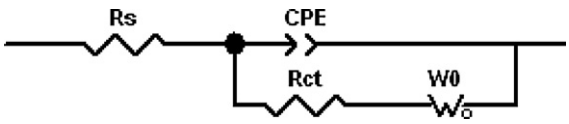

Fig. 8. Equivalent circuit.

Table 2
Results of electrochemical impedance.

Material	R_s (Ω)	R_{ct} (Ω)
$Li_3V_2(PO_4)_3$/C	12.18	1649
MgO coated $Li_3V_2(PO_4)_3$/C	12.56	302.7

by a depressed semicircle in the high-middle frequency region and a straight line in the low frequency region. The intercept impedance on the Z' axis represents the resistance of solvent, and R_s is used to denote it in equivalent circuit. The semicircle is attributed to the charge-transfer resistance of electrochemical reaction and the line to the diffusion controlled Warburg, and the Rct and W_0 are used to denote them in the equivalent circuit, respectively. A constant phase element CPE is placed to represent the double layer capacitance and passivation film capacitance [15,23], and the capacitance resistance is so small to be negligible. The fitting results are shown in Table 2. It can be understood that the resistance of the solvent (R_s) has no large change for pristine $Li_3V_2(PO_4)_3$/C and MgO coated $Li_3V_2(PO_4)_3$/C electrodes. This is because the same electrolyte is used when the test cells are assembled. The charge-transfer resistance at MgO coated $Li_3V_2(PO_4)_3$/C electrode is much less than that at pristine $Li_3V_2(PO_4)_3$/C, indicating that the coating is more favorable for the insertion and de-insertion of lithium ions during the charge and discharge process. This result is similar to that of ZrO_2 coated $LiFePO_4$ [18].

The initial CV curves for pristine $Li_3V_2(PO_4)_3$/C and MgO of 4.5 mol% coated $Li_3V_2(PO_4)_3$/C are shown in Fig. 9. Both curves show a similar profile, and there are four oxidation peaks and three reduction peaks in CV curves, which indicate that the reaction behavior does not change during the lithium extraction/insertion process for the coated electrode. As shown in Fig. 8, the four oxidation peaks of pristine $Li_3V_2(PO_4)_3$/C are located at about 3.68, 3.74, 4.14 and 4.59 V, respectively, and three reduction peaks are located around 3.51, 3.58 and 3.88 V, respectively. The extraction and intercalation potentials are similar to those reported by Saidi et al. [24]. However, in the case of MgO coated $Li_3V_2(PO_4)_3$/C electrode, the oxidation peaks shift down to 3.66, 3.73, 4.13,and

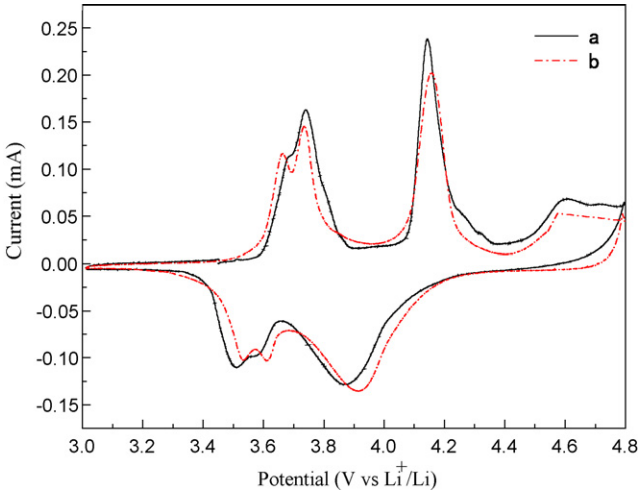

Fig. 9. CV curves of $Li_3V_2(PO_4)_3$/C (a) and 4.5 mol% MgO coated $Li_3V_2(PO4)_3$/C (b).

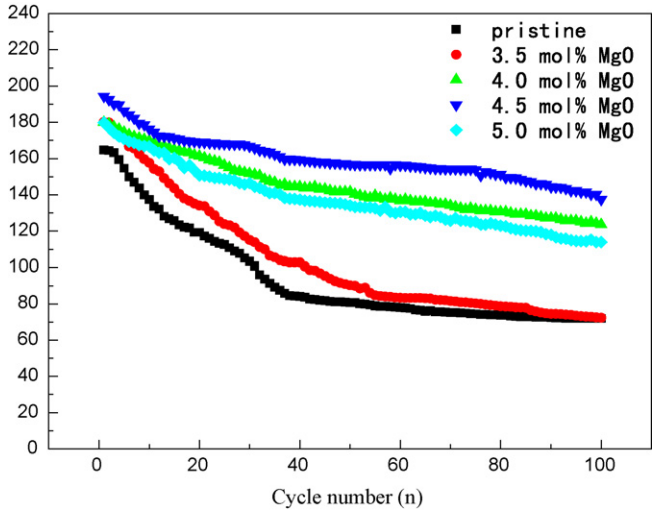

Fig. 10. Discharge capacity *vs.* cycles for $Li_3V_2(PO_4)_3$/C and different amount of MgO coated $Li_3V_2(PO4)_3$/C at 40 mA g^{-1}.

4.57 V, respectively, while the reduction peaks shift up to 3.53, 3.61 and 3.92 V, respectively. Namely, all the anodic peaks shift to the higher potentials and cathodic peaks shift to lower potentials, and then the potential differences between anodic peaks and cathodic peaks become smaller. The well-defined peaks and smaller value of potential interval show the enhancement of electrode reaction reversibility.

The cycling performances are presented in Fig. 10 for pristine $Li_3V_2(PO_4)_3$/C and the MgO coated $Li_3V_2(PO_4)_3$/C samples with various MgO amount. From Fig. 10, it can be seen that all the MgO coated $Li_3V_2(PO_4)_3$/C samples exhibit higher initial discharge capacity than pristine sample, which may be due to the formation of a surface solid solution $Li_3Mg_xV_{2-x}(PO_4)_3$. In the case of MgO coated samples, low content MgO does not evidently improve the cycling performance. For example, the discharge capacity of MgO of 3.5 mol% coated $Li_3V_2(PO_4)_3$/C is similar to that of pristine $Li_3V_2(PO_4)_3$/C after 100 cycles, and it is probable that the small amount MgO coated on $Li_3V_2(PO_4)_3$/C is dissolved with increasing the cycle number. With increasing the amount of MgO, the samples exhibit excellent cycling performances. Especially for MgO of 4.5 mol% coated sample, the initial discharge capacity is 194.4 mAh g^{-1}, which is close to the theoretical discharge capacity of 197 mAh g^{-1}. Upon cycling, the discharge capacity degrades slowly and remains 137.5 mAh g^{-1} after 100 cycles, and the capacity retention is 70.73%, which is higher than that of pristine $Li_3V_2(PO_4)_3$/C, 43.7%. The phenomenon may be related to the following factors: (1) MgO acts as a protective layer to prevent the electro-active material core from direct contact with the electrolytes, and thus improves structural stability; (2) MgO coated suppresses the increase in resistances caused by repeated insertion–extraction of lithium ions during charge/discharge processes; (3) MgO coated enhances the reversibility of electrode reaction. However, when the amount of MgO is increased to 5.0 mol%, the initial discharge capacity and cycling stability are descended, which may be due to excessive amount of MgO. MgO of 4.5 mol% coated on $Li_3V_2(PO_4)_3$/C is reasonable to improve cycling performance.

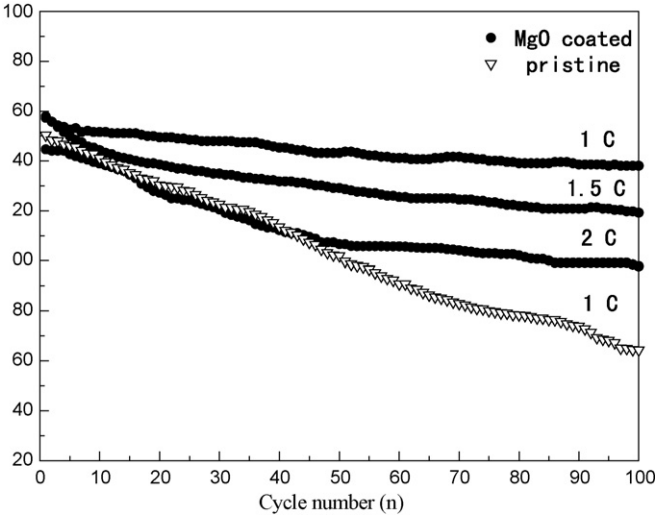

Fig. 11. Discharge capacity *vs.* cycles for $Li_3V_2(PO_4)_3$/C and 4.5 mol% MgO coated $Li_3V_2(PO4)_3$/C at different current density.

Rate performances of pristine $Li_3V_2(PO_4)_3$/C and MgO of 4.5 mol% coated $Li_3V_2(PO_4)_3$/C are given in Fig. 11. At 1C current density, it is obvious that the cyclability of MgO coated sample is better than that of pristine $Li_3V_2(PO_4)_3$/C, the initial discharge capacity is 157.81 mAh g^{-1} and the discharge capacity remains 137.02 mAh g^{-1} after 100 cycles, but the discharge capacity of pristine $Li_3V_2(PO_4)_3$/C degrades sharply and falls from the initial 150.33 mAh g^{-1} to 64.39 mAh g^{-1} after 100 cycles. In addition, the cyclability of MgO of 4.5 mol% coated sample at 1.5C and 2C rates was tested, respectively. As shown in Fig. 10, MgO coated sample exhibits good rate performance. When current density is increased to 1.5C and 2C, the initial discharge capacity still reaches 157.29 mAh g^{-1} and 144.64 mAh g^{-1}, respectively, and the discharge capacity falls to 119.27 mAh g^{-1} and 97.79 mAh g^{-1} after 100 cycles, respectively.

4. Conclusions

MgO coating was performed on the surface of $Li_3V_2(PO_4)_3$/C. HRTEM image confirms that a MgO layer of 2.0–2.5 nm is coated on the surface of $Li_3V_2(PO_4)_3$/C particles. The MgO nanocoating improves the structural stability of the cathode material, decreases the interface charge transfer resistance and enhances the reversibility of electrode reaction, and thus, remarkably improves the electrochemical performance of the cathode material. Both the initial discharge capacity and the cyclability of $Li_3V_2(PO_4)_3$/C can be notably improved, particularly the rate performance. The nanocoating method could be a promising approach to improve the electrochemical properties of $Li_3V_2(PO_4)_3$/C cathode material.

Acknowledgment

This work was financially supported by the National Natural Science Foundation of China (Grant No. 20771100).

References

[1] T. Kerr, J. Gaubicher, L.F. Nazar, Electrochem. Solid State Lett. 3 (2000) 460.
[2] X.F. Ouyang, M. Lei, S.Q. Shi, C.L. Luo, D.S. Liu, D.Y. Jiang, Z.Q. Ye, M.S. Lei, J. Alloys Compd. 476 (2009) 462.
[3] C.S. Sun, Z. Zhou, Z.G. Xu, D.G. Wang, J.P. Wei, X.K. Bian, J. Yan, J. Power Sources 193 (2009) 841.
[4] N.N. Bramnik, K. Nikolowski, D.M. Trots, H. Ehrenberg, Electrochem. Solid State Lett. 11 (6) (2008) A89.
[5] S.-W. Kim, J. Kim, H. Gwon, K. Kang, J. Electrochem. Soc. 156 (8) (2009) A635.
[6] T. Shiratsuchi, S. Okada, T. Doi, J.-I. Yamaki, Electrochim. Acta 54 (2009) 3145.
[7] X.J. Zhu, Y.X. Liu, L.M. Geng, L.B. Chen, H.X. Liu, M.H. Cao, Solid State Ionics 179 (2008) 1679.
[8] Q.Q. Chen, J.M. Wang, Z. Tang, W.C. He, H.B. Shao, J.Q. Zhang, Electrochim. Acta 52 (2007) 5251.
[9] H. Huang, T. Faulkner, J. Barker, M.Y. Saidi, J. Power Sources 189 (2009) 748.
[10] A.K. Padhi, K.S. Nanjundaswamy, J.B. Goodenough, J. Electrochem. Soc. 144 (1997) 1188.

[11] S.Q. Liu, S.C. Li, K.L. Huang, Z.H. Chen, Acta Phys. Chim. Sin. 23 (4) (2007) 537.
[12] M.M. Ren, Z. Zhou, Y.Z. Li, X.P. Gao, J. Yan, J. Power Sources 162 (2006) 1357.
[13] Q. Kuang, Y.M. Zhao, X.N. An, J.M. Liu, Y.Z. Dong, L. Chen, Electrochim. Acta 55 (2010) 1575.
[14] S.Q. Liu, S.C. Li, K.L. Huang, B.L. Gong, G. Zhang, J. Alloys Compd. 450 (2008) 499.
[15] C.X. Chang, J.F. Xiang, X.X. Shi, X.Y. Han, L.J. Yuan, J.T. Sun, Electrochim. Acta 53 (2008) 2232.
[16] L.J. Wang, X.C. Zhou, Y.L. Guo, J. Power Sources 195 (2010) 2844.
[17] T. Jiang, Y.J. Wei, W.C. Pan, Z. Li, X. Ming, G. Chen, C.Z. Wang, J. Alloys Compd. 488 (2009) L26.
[18] H. Liu, G.X. Wang, D. Wexler, J.Z. Wang, H.K. Liu, Electrochem. Commun. 10 (2008) 165.
[19] M.Y. Saidi, J. Barker, H. Huang, J.L. Swoyer, G. Adamson, Electrochem. Solid State Lett. 5 (2002) A149.
[20] M. Mladenov, R. Stoyanova, E. Zhecheva, S. Vassilev, Electrochem. Commun. 3 (2001) 410.
[21] R. Alcantara, M. Jaraba, P. Lavela, J.L. Tirado, J. Electroanal. Chem. 566 (2004) 187.
[22] Y.Z. Li, Z. Zhou, X.P. Gao, J. Yan, Electrochim. Acta 52 (2007) 4922.
[23] G.X. Wang, L. Yang, Y. Chen, Electrochim. Acta 50 (2005) 4649.
[24] M.Y. Saidi, J. Barker, H. Huang, J.L. Swoyer, G. Adamson, J. Power Sources 119–121 (2003) 266.